A CONSTITUTIVE MODEL FOR THE ANELASTIC BEHAVIOR OF ADVANCED HIGH STRENGTH STEELS

A. Torkabadi*, P. van Liempt†, V.T. Meinders* and A.H. van den Boogaard*

* University of Twente, Faculty of Engineering Technology
Chair of Nonlinear Solid Mechanics
P.O. box 217-7500 AE Enschede- The Netherlands
e-mail: a.torkabadi@utwente.nl

† Tata Steel Research, Development & Technology
P.O. box 10000 (3G37)-1970 CA IJmuiden- The Netherlands
e-mail: peter.van-Liempt@tatasteel.com

Key words: Anelasticity, Dislocations, Advanced High Strength Steels, Springback.

Abstract. In this work a physically based model describing the anelastic behaviour and nonlinear unloading in Advanced High Strength Steels (AHSS) is proposed. The model is fitted to the experimental data obtained from uni-axial tests on a dual-phase high strength steel grade (HCT780). The results show a good agreement between the model and the experimental data.

1 INTRODUCTION

Automotive industry is increasing the use of Advanced High Strength Steels (AHSS) to reduce the weight of vehicles. The major hurdle in employing AHSS is not the limited formability but the dimensional control, mainly due to a phenomenon called springback. The accuracy of springback prediction can be improved by a better prediction of the stress states in the part during the deformation and the material behaviour during unloading [1]. While most researchers have been trying to improve the former by introducing and employing novel plasticity models, little attention has been paid to the latter. Historically, in classic elasto-plastic modelling, the unloading of the material is assumed to be linearly elastic (Hooke's law) with a slope equal to the handbook value of the E-modulus (e.g. 210 GPa for steel). However, experimental observations have shown that this assumption is not realistic. It has been widely observed that the loading/unloading stress-strain curves of plastically deformed metals are nonlinear, showing a hysteresis behaviour during loading/unloading cycles [2-4]. Additionally, the average unloading modulus, the slope of the straight line connecting the stress point at the start of unloading to the point at zero stress, decreases with increasing plastic deformation. As a result, the springback would be larger than that predicted by FEM using the initial E-modulus to model the unloading behaviour. This has been commonly attributed to 'E-modulus degradation' in the literature; even though, 'E-modulus degradation' or similar terms are inaccurate denominations since the elastic modulus is a result of interatomic interactions and a fundamental material property which is independent from the plastic strain. Anelasticity mechanisms and springback in metals have been studied independently for the past years. However, no anelastic material model for springback simulations pre-exists.

The dislocation based anelasticity is known to be the root cause of such phenomena [2, 5, 6]; as a matter of fact, in addition to the purely elastic strain, extra dislocation based micro-mechanisms are contributing to the reversible strain of the material which results in the nonlinear unloading/reloading behaviour and the reduction of the average unloading/reloading modulus. This extra reversible strain is the so called anelastic strain. In this work, an anelastic model is proposed to describe the nonlinear unloading behaviour after plastic deformation. In this framework, the total reversible strain is assumed to be partially elastic and partially anelastic. The anelastic strain recovered upon unloading is measured by subtracting the purely elastic strain (obtained by Hooke's law) from the total recovered strain. Based on that, a model is developed that predicts the magnitude of the recovered anelastic strain upon unloading at each stress as a function of the equivalent plastic strain. The model is fitted to experimental data obtained from uni-axial tests on a dual-phase high strength steel grade (HCT780).

2 THE MODEL

According to Mott [7] and Friedel [8], the magnitude of the anelastic strain resulted from a shear stress τ acting on a dislocation segment is given by

$$\gamma = NbA \tag{1}$$

where *N* is the number of dislocation segments with length *l* per unit volume, *b* is the Burgers vector and *A* is the area that is swapped by the dislocation segment traveling between its initial state to its new equilibrium position. In a material the dislocation segment length is a distribution. As an approximation, the segment length *l* can be taken as the average segment length in the material. A relation between the dislocation density ρ, the number of dislocation segments *N* and the average dislocation segment length *l* holds according to

$$\rho = Nl \tag{2}$$

Equation (1) consists of a constant 'b' and two independent variables '*N*' and '*A*'. An expression for *A* has been derived by van Liempt [9] giving the shear anelastic strain as a function of shear stress according to

$$\gamma = Nb\frac{G^2b^2\sin^{-1}\left(\frac{\tau l}{Gb}\right) - Gbl\tau\sqrt{1-\frac{\tau^2 l^2}{G^2b^2}}}{4\tau^2} \tag{3}$$

where *G* is the shear modulus of the material and τ is the shear stress acting on the dislocation segment. The area that is swapped by the dislocation segment during loading from 0 reaches its maximum equal to $\frac{1}{8}\pi l^2$ (area of a semi-circle with diameter of *l*) when $\tau = \tau_c = \frac{Gb}{l}$ (τ_c is the critical shear stress of the Frank-Read source). Beyond this point the loop expands rapidly and the strain becomes irreversible. This is the point when plastic deformation occurs according to the Frank-Read mechanism. With that respect a dimensionless parameter $s = \frac{\tau}{\tau_c}$, $0 \le s \le 1$, can be utilized in Equation (3) yielding

$$\gamma = Nbl^2 \frac{sin^{-1}(s) - s\sqrt{1-s^2}}{4s^2} \tag{4}$$

At any point during loading/unloading (at relatively low temperatures), as long as $\tau < \frac{Gb}{l}$ ($s < 1$), it can be assumed that *N* stays constant. *N* only evolves when the population of dislocations increases during the plastic deformation or decreases by dislocation annihilation processes (i.e. dislocation climb) at high temperatures and stresses.

In a material prior to plastic deformation, the value of *N* is larger than 0 due to the fact that there are always dislocations in the material which leads to pre-yield anelastic behaviour. Upon the onset of plastic deformation, the population of the dislocations significantly increases in the material by the activation of dislocation multiplication mechanisms such as the Frank-Read source.

In order to evaluate the population of the dislocations and the average dislocation segment length, experimental methods can be employed to estimate the dislocation density. However, these methods are often unreliable and very localized which makes extrapolation of the results to the entire material difficult. Instead, the effect of dislocation density increase on macroscopic properties of the material, namely the flow stress, can be used as a measure to estimate the dislocation density in the material.

The Taylor equation is one of the oldest expressions relating the flow stress of a material to its dislocation density [10] according to

$$\sigma_f = \sigma_0 + \bar{M}\alpha Gb\sqrt{\rho} \tag{5}$$

where $\bar{M}$ is the Taylor factor, α is the dislocation strengthening parameter and a material related constant, *G* is the shear modulus of the material, ρ is the dislocation density and σ_0 is the flow stress of the material in the absence of dislocation interactions. It should be noted that σ_0 is a fictional value as in reality there are always dislocations in the material. To overcome this problem Equation (5) can be rewritten as

$$\sigma_f = \sigma_y + \bar{M}\alpha Gb\left(\sqrt{\rho} - \sqrt{\rho_0}\right) \tag{6}$$

where ρ_0 is the dislocation density of the material when it becomes plastically deformed at σ_y.

Rewriting Equation (6) yields an expression for dislocation density evolution as a function of hardening behaviour of the material according to

$$\rho = \left(\frac{\sigma_f - \sigma_y}{\bar{M}\alpha Gb} + \sqrt{\rho_0}\right)^2 \tag{7}$$

Making use of Equation (2) and (7), Equation (1) can be written as

$$\gamma = NbA = \frac{\rho}{l}bA = \left[\left(\frac{\sigma_f - \sigma_y}{\bar{M}\alpha Gb} + \sqrt{\rho_0}\right)^2\right]\frac{bA}{l} \tag{8}$$

The presence of the initial dislocation density ρ_0 in the material before the initiation of the plastic deformation at σ_y will result in a pre-yield anelastic shear strain of

$$\gamma_{pre} = \frac{\rho_0}{l}bA \tag{9}$$

With that respect, the total anelastic strain in the material can be expressed as the sum of the pre-yield anelasticity due to the pre-existing dislocations and anelasticity resulted from the newly stored dislocations upon work hardening of the material.

The anelastic resolved shear strain can be converted to the macroscopic uniaxial strain using the Taylor factor

$$\varepsilon^{an} = \frac{1}{\bar{M}}\left[\left(\frac{\sigma_f - \sigma_y}{\bar{M}\alpha G b} + \sqrt{\rho_0}\right)^2\right]\frac{bA}{l} \tag{10}$$

As it was mentioned earlier, *A* is a stress dependent parameter which varies between 0 at $\sigma = 0$ to $\frac{\pi}{8}l^2$ at $\sigma = \sigma_f$. During the plastic deformation the average value of *A* stays constant at its maximum and the magnitude of the anelastic strain increases as a function of work hardening due to an increase of dislocation density according to Equation (10).

Hence the maximum anelastic strain that may be stored in or recovered from the material can be estimated by replacing *A* in Equation (10) with $\frac{\pi}{8}l^2$ according to

$$\varepsilon_{max}^{an} = \frac{1}{\bar{M}}\left(\frac{\sigma_f - \sigma_y}{\bar{M}\alpha G b} + \sqrt{\rho_0}\right)^2\frac{b\pi l}{8} \tag{11}$$

According to Equation (11) the evolution of the anelastic strain is given as a function of the work hardening behaviour of the material and several material constants. The material constants can be casted into a single parameter *K*

$$\varepsilon_{max}^{an} = \left[K\left(\sigma_f - \sigma_y\right) + \sqrt{\varepsilon_{pre}^{an}}\right]^2 \tag{12}$$

The value of *K* can be determined by fitting Equation (12) to the experimental data. For that, the evolution of ε_{max}^{an} as a function of flow stress should be determined. This can be done by sequential unloading/reloading of the material after some work hardening (see Figure 1). Considering that the total reversible strain is partially elastic and partially anelastic, the contribution of the anelastic strain can be determined by subtracting the elastic strain from the entire recovered strain

$$\varepsilon^{an} = \varepsilon^{reversible} - \varepsilon^{e} = \varepsilon^{reversible} - \frac{\sigma_f}{E} \tag{13}$$

where *E* is the theoretical value of the *E*-modulus at room temperature. The calculation of the anelastic strain from Equation (13) is based on the assumption that the total anelastic strain stored in the material during loading would be recovered entirely after unloading to zero stress.

After determining the value of *K*, Equation (10) can be rewritten by inserting *K* and the expression for *A* as

$$\varepsilon^{an} = \left(\left[K\left(\sigma_f - \sigma_y\right) + \sqrt{\varepsilon_{pre}^{an}}\right]^2\right)\left[\frac{2}{\pi}\frac{sin^{-1}(s) - s\sqrt{1-s^2}}{s^2}\right] \tag{14}$$

Hence, the anelastic strain in the material can be expressed by two independent functions in the parentheses and the brackets. All the material dependent parameters are casted into *K* which can be determined from experimental data. For practical reasons hereafter the function in the parentheses is referred to as the ***f*** function and the function in the brackets the ***g*** function. ***f*** is a function of flow stress in the material and evolves when the density of dislocation increases due to plastic deformation. The ***g*** function only evolves when the stress is below the flow stress of the material and is a function of the current state of the stress. During plastic deformation where $s = 1$, $g(s = 1) = 1$ hence Equation (14) transcends into Equation (12). Therefore, the anelastic strain rate below the flow stress and during plastic deformation can be expressed as

$$\dot{\varepsilon}^{an} = f.\dot{g} \quad \sigma < \sigma_f$$

$$\dot{\varepsilon}^{an} = \dot{f} \quad \sigma = \sigma_f$$

The term $(\sigma_f - \sigma_y)$ in the $\boldsymbol{f}$ function can be replaced with a hardening law that is suitable for the material under study. Consequently the $\boldsymbol{f}$ function can be expressed as a function of equivalent plastic strain.

As the maximum amount of anelastic strain increases according to Equation (12), the effective unloading modulus decreases. Knowing the evolution of the anelastic strain as a function of flow stress, the reduction in the average unloading modulus can be easily modelled. The average unloading modulus E_A can be written as the sum of elastic (E) and average anelastic (Θ_A) modulus in series

$$\frac{1}{E_A} = \frac{1}{E} + \frac{1}{\Theta_A} = \frac{1}{E} + \frac{\varepsilon_{max}^{an}}{\sigma_f} \tag{15}$$

Making use of Equation (12), Equation (15) can be rewritten as

$$E_A = \frac{E\sigma_f}{\sigma_f + E\left[K(\sigma_f - \sigma_y) + \sqrt{\varepsilon_{pre}^{an}}\right]^2} \tag{16}$$

Various authors have developed models such as Equation (16) to predict the variation of the average unloading modulus. They have reported a significant improvement in springback prediction by adopting a variable unloading modulus [11-13].

3 EXPERIMENTAL PROCEDURE

This study was performed on HCT780 steel grade provided by Tata steel. The samples were cut according to ASTM E8 standard from a steel sheet with a thickness of 1 mm. The tensile tests were conducted using an Instron 5980 electromechanical universal testing machine and the strain was measured using a clip-on extensometer.

The controller was programmed to load the specimen to 1% nominal strain (engineering strain) and then unload to zero stress. Immediately after the first loading/unloading cycle, the specimen was reloaded to 2% of nominal strain and unloaded again. This procedure was repeated with increments of 1% straining until 8% of nominal strain was achieved. The loading/unloading cycles were carried out at a constant crosshead speed of 5 mm/min.

4 EXPERIMENTAL RESULTS

The stress-strain curve obtained from the cyclic loading/unloading experiment is shown in Figure 1. Note that the values of the true strain are slightly lower than the nominal strain that was prescribed.

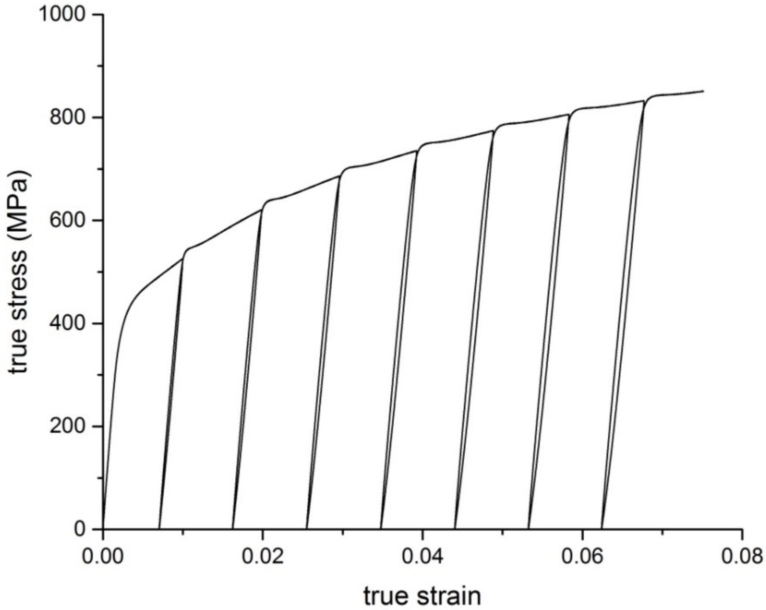

Figure 1 Stress-strain curve obtained from cyclic unloading/reloading experiment.

In order to fit Equation (12) to the experimental data, the anelastic strain should be plotted as a function of flow stress. However, first the yield stress σ_y has to be determined. The value of σ_y can be approximated from the Kocks-Mecking plot [9]. In the Kocks-Mecking plot the first differential of the stress-strain curve is plotted against the stress. At the yield stress the slope of the Kocks-Mecking plot changes abruptly. The details on the determination of the yield stress from the Kocks-Mecking plots are discussed in [9]. It is worth nothing that this value for the yield stress is different from the Rp02 value commonly used in the handbooks.

From the Kocks-Mecking plots, the average value of the yield stress was found to be approximately 440 MPa. Substituting $\sigma_y = 440$ MPa into Equation (12), the model can be fitted to the experimental data taking K and ε_{pre}^{an} as the fitting parameters (Figure 2).

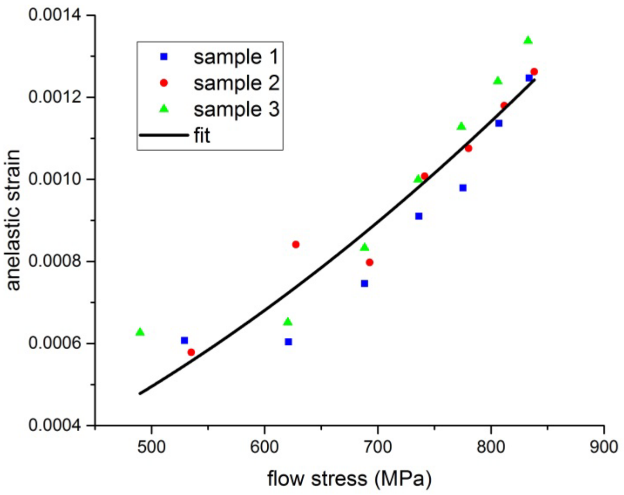

Figure 2 The evolution of the anelastic strain as a function of flow stress fitted with Equation (12).

The values of $\mathrm{K} = 3.84 * 10^{-5}$ and $\varepsilon_{\mathrm{pre}}^{\mathrm{an}} = 3.98 * 10^{-4}$ were obtained from curve fitting using the least squares method. These values can be used in Equation (14) to describe the anelastic behaviour of this material. The quadratic relation between the work hardening and the anelastic strain of the material given in Equation (12) fits well with the experimental data (R^2=0.89797). Having the values of K and ε_{pre}^{an}, the unloading curves can be constructed by adding the anelastic strain from Equation (14) to the purely elastic strain $(\frac{\sigma}{E})$. The analytical plots for the anelastic model are plotted with experimental data in Figure 3-a for different unloading stages. A magnified view of a selected unloading/reloading curve is shown in Figure 3-b and the unloading curve obtained from the anelastic model is compared with purely elastic unloading and unloading with an average modulus obtained from Equation (16).

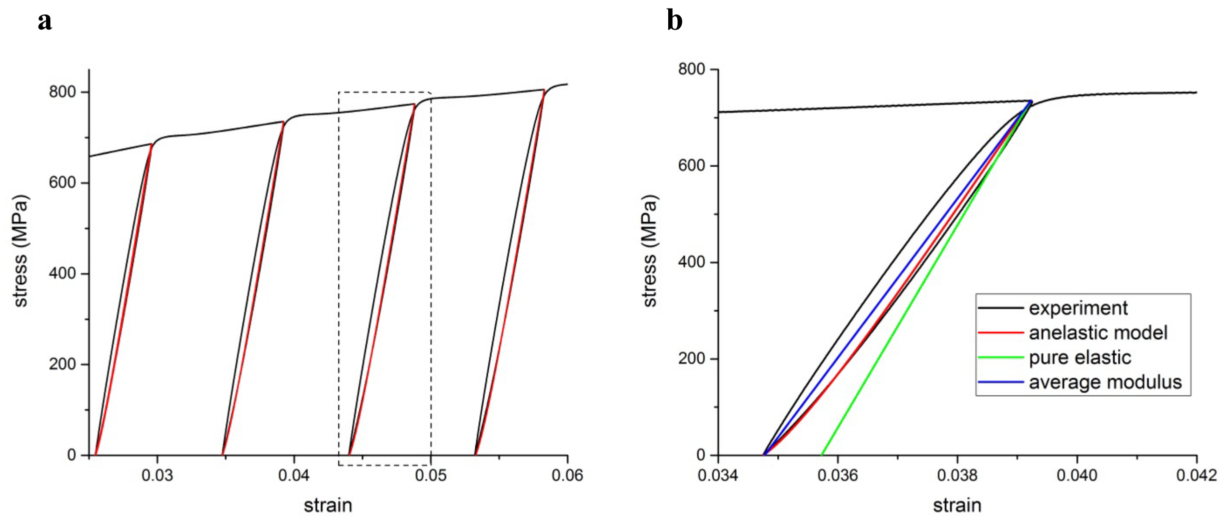

Figure 3 Stress-strain response of HCT780 (a) calculated unloading curve (red) and the experimental data (black); (b) magnified view of the selected region.

As can be seen in Figure 3-b, the predicted unloading curve using the anelastic model is very well in agreement with the experimental data; whereas, the unloading path obtained by purely elastic unloading and unloading using the average modulus tend to underpredict and overpredict the recovered strain respectively.

It should be noted that a lattice friction stress of 25 MPa was considered to build the unloading stress-strain curves using the anelastic model. This is due to the fact that upon unloading, in absence of external force, the movement of dislocation is impeded by the resistance of the lattice. During unloading when the stress approaches zero, there is no motive force to move the dislocation further.

5 CONCLUSION

The proposed model is well capable of describing the anelastic behaviour and nonlinear unloading in AHSS. As the material deforms plastically, the magnitude of the anelastic strain evolves increasingly. This results in a reduction of the average unloading modulus. The evolution of anelastic strain corresponds to the dislocation density in the material and can be related to the hardening behaviour of the material through the Taylor's relation. The value of K is physically meaningful. However, it represents an effective value for the material and can differ with the value obtained from local measurements in the material.

REFERENCES

1. Wagoner, R.H., H. Lim, and M.-G. Lee, *Advanced Issues in springback.* International Journal of Plasticity, 2013. **45**(0): p. 3-20.
2. Cleveland, R.M. and A.K. Ghosh, *Inelastic effects on springback in metals.* International Journal of Plasticity, 2002. **18**(5–6): p. 769-785.
3. Eggertsen, P.A., K. Mattiasson, and J. Hertzman, *A Phenomenological Model for the Hysteresis Behavior of Metal Sheets Subjected to Unloading/Reloading Cycles.* Journal of Manufacturing Science and Engineering, 2011. **133**(6): p. 061021-061021.
4. Sun, L. and R.H. Wagoner, *Complex unloading behavior: Nature of the deformation and its consistent constitutive representation.* International Journal of Plasticity, 2011. **27**(7): p. 1126-1144.
5. Luo, L. and A.K. Ghosh, *Elastic and Inelastic Recovery After Plastic Deformation of DQSK Steel Sheet.* Journal of Engineering Materials and Technology, 2003. **125**(3): p. 237-246.
6. Benito, J.A., et al., *Change of Young's modulus of cold-deformed pure iron in a tensile test.* Metallurgical and Materials Transactions A, 2005. **36**(12): p. 3317-3324.
7. Mott, N.F., *CXVII. A theory of work-hardening of metal crystals.* The London, Edinburgh, and Dublin Philosophical Magazine and Journal of Science, 1952. **43**(346): p. 1151-1178.
8. Friedel, J., *XLVI. Anomaly in the rigidity modulus of copper alloys for small concentrations.* The London, Edinburgh, and Dublin Philosophical Magazine and Journal of Science, 1953. **44**(351): p. 444-448.
9. van Liempt, P. and J. Sietsma, *To be published.* 2015.
10. Taylor, G.I., *The Mechanism of Plastic Deformation of Crystals. Part I. Theoretical.* Proceedings of the Royal Society of London. Series A, Containing Papers of a Mathematical and Physical Character, 1934. **145**(855): p. 362-387.
11. Morestin, F. and M. Boivin, *On the necessity of taking into account the variation in the Young modulus with plastic strain in elastic-plastic software.* Nuclear Engineering and Design, 1996. **162**(1): p. 107-116.
12. Ghaei, A., D.E. Green, and A. Taherizadeh, *Semi-implicit numerical integration of Yoshida–Uemori two-surface plasticity model.* International Journal of Mechanical Sciences, 2010. **52**(4): p. 531-540.
13. Li, X., et al., *Effect of the material-hardening mode on the springback simulation accuracy of V-free bending.* Journal of Materials Processing Technology, 2002. **123**(2): p. 209-211.